Journal of Optoelectronics and Advanced Materials Vol. 6, No. 3, September 2004, p. 865 - 874

THE SINGLE STEP INVERSE CALCULATIONS OF THE EFFECTIVE PAIR POTENTIALS FOR LIQUID LITHIUM

S. Dalgic*, S. S. Dalgic

Department of Physics, Trakya University, 22030 Edirne, Turkey

It is presented the revised effective pair potentials for liquid lithium extracted from experimental structure data using the inverse method, which is based on the variational modified hypernetted-chain (VMHNC) integral equation theory of liquids. The reliability of the revised potential is supported by a comparison the neutral pseudoatom potential at several thermodynamic states. Although the single-step VMHNC inversion yields acceptable results for the characteristic features of the density dependence of the revised potentials for liquid lithium, the difference in the medium behaviour of the Li potential is a cause of concern. This discrepancy and the limitations of the approximate theories in the inverse calculations have been discussed with the possible improvements.

(Received June 2, 2004; accepted June 22, 2004)

Keywords: Liquid lithium, Inverse method, Effective potentials, Variational modified hypernetted chain theory

1. Introduction

The so-called inverse problem, for deriving the pair potentials from the the experimental structure factor has been originally proposed by Johnson and March [1,2]. One of the route followed to derive the effective pair potentials from measured structural data which is based on the formalism developed by de Angelis and March [3] from the Born-Green-Yvon hierarchy has been utilized by a number of workers [4]. This is the so-called approximate inverse formula. Another route is the inversion scheme based on the Ornstein-Zernike equation or approximate closures that relate the structure factor $S(k)$ to the pair potential $\phi(r)$ in a simple fashion. Therefore inversion schemes that rely on such integral equation theories, as the Percus - Yevick (PY) [5], Hypernetted Chain (HNC), Mean Spherical approximation (MSA) and Modified Hypernetted Chain (MHNC) equation [6] are often called "single step" inversions. This inverse problem is the focus of this paper. It has been claimed [7,8] that MHNC relation is more efficient than other theories in both the direct and inverse problem. There are different versions of MHNC equation which is related to the actual choice of the bridge functions and different criteria to determine the parameters defining them. These are reference hypernetted chain (RHNC) [9] and the variational modified hypernetted chain theory (VMHNC) [10]. In the "multi-step", predictor-corrector inversions the molecular-dynamic simulation is also used by many investigators in cases where the structure data need to be modified [7,11 – 16].

In this work, we investigate the validity of the VMHNC approximation in the inverse calculations of liquid lithium. In connection with , researchers show that VMHNC is widely used to predict static structure factors and thermodynamic properties of liquid metals in direct calculations [17- 22]. Recent molecular dynamic (MD) simulations [18] have shown that dynamical properties of liquid lithium near the melting and the triple point are in very good agreement with experimental data using an interionic pair potential derived from the neutral pseudoatom (NPA) method [23,24]. It has been reported that other effective pair potentials used in MD simulations of liquid Li [25] are significantly closer to the results of Canales *et al.* [18]. For these reasons that we choose the VMHNC integral-equation method based on the Ornstein-Zernike (OZ) equation for our inverse calculations. Our first aim is to derive the pair potentials for liquid lithium from experimental struc-

* Corresponding author: dseyfe@yahoo.co.uk

ture data at several thermodynamic states. For this purpose, the MHNC equation is solved for a fluid of particles interacting through the revised potential with variational criterion. In order to test the accuracy of the inversion scheme and the reliability of the revised potential, we have compared our results with those obtained from the NPA method and model pseudopotentials recently proposed by Fiolhais et al. [26]. We have also analysed the trends in the liquid structure of Li through the revised potentials. The corresponding thermodynamic properties with the presented inversion scheme follow the expected trends with decreasing density. The results show that VMHNC liquid state theory is yielding the acceptable results in the inverse problem to extract the potentials $\beta\phi(r)$ for liquid lithium within the limit of experimental accuracy, than previously obtained from experimental data. However, we should noticed that there is a difference in the medium behaviour of the Li potential at intermediate-range distances when it compares with the NPA potential. Some researchers have been noted that the universality of ansatz of Rosenfeld-Ashcroft (RA) does not hold for some thermodynamic states in order to describe the interactions at intermediate range [27, 28]. This work is another test about the validity of universality ansatz in the inverse calculations for liquid metals at their melting points. Although we are currently engaged in inverting the diffraction data on S(k) to determine a pair potential for direct comparison with the NPA potential, we have suggested a possible improvement for the single-step revised potentials. In the case of the thermodynamic state near its melting , the revised potential has been performed with the revised bridge function extracted from the MHNC equation using a new closure proposed by Poll, Ashcroft and de Witt (PAD) [27]. Thus we have shown the revised bridge functions obtained by the suggested procedure can be used for improving the inverse calculations of liquid metals at their melting points which is based on the integral equations.

The paper is organised as follows, In section 2 we summarise the theoretical methods applied in this work. In the same section we give a brief description of the inversion schemes considered. In section 3 we present the results of our calculations. First, we give the details of the inversion of experimental structure data. This is followed by a comparison with NPA potentials. Finally, the calculated thermodynamic properties are given by comparing both NPA and experimental results.

2. Formalism

In the integral equation approach, the effective pair potential $\beta\phi(r)$ has been obtained using the exact closure in terms of the pair distribution function g(r), the direct correlation function c(r) and bridge function B(r). The exact closure is given by

$$\beta\phi(r) = g(r) - c(r) - \ln g(r) - 1 + B(r) \tag{1}$$

In the inverse calculations, the pair potential can be obtained in a straight-forward manner from given experimental structure data $S_{exp\,t}(k)$ using Eq.(1). The experimental pair distribution function $g_{exp\,t}(r)$ can be obtained from $S_{exp\,t}(k)$ by the Fourier transformation

$$g_{exp\,t}(r) = 1 + \frac{1}{2\pi^2 \rho r}\int (S_{exp\,t}(k) - 1)k \sin(kr)\,dk \tag{2}$$

where ρ is the number density of ions. The experimental direct correlation function $c_{exp\,t}(r)$ can be found from the same $S_{exp\,t}(k)$ directly using the Ornstein-Zernike (OZ) equation which for an isotropic, homogenous system can be written as

$$g(r) - 1 - c(r) = \rho\int (g(|r - r'|) - 1)c(r')\,dr', \tag{3}$$

together with Eq. (1). , $c_{exp\,t}(r)$ can be given by

$$c_{exp\,t}(r) = \frac{1}{2\pi^2 \rho r}\int \left(1 - \frac{1}{S_{exp\,t}(k)}\right)k \sin(kr)\,dk. \tag{4}$$

We consider two different inversion scheme based on the integral equations. In order to extract the revised potential with Eq.(1), the parameterised hard-sphere bridge function and the extracted bridge function have been used. The parameterised hard-sphere bridge function is used for the VMHNC based on inverse calculations to extract the effective pair potential which is given by

$$\beta\phi_{VMHNC}(r) = g_{expt}(r) - c_{expt}(r) - \ln g_{expt}(r) - 1 + B_{HS}^{PY}(r,\eta) \tag{5}$$

This is so called the VMHNC based on inversion scheme. Here $B(r) = B_{HS}^{PY}(r,\eta)$, appropriates to hard spheres (HS) within the Percus-Yevick (PY) approximation and determines the single free parameter η, hard sphere packing fraction , by imposing the requirement of thermodynamic consistency between the virial and compressibility routes. This is so called VMHNC equation.. In order to choose η as a function of the thermodynamic state, that is, $\eta = \eta(\beta,\rho)$, the VMHNC variational criterion takes the form

$$\frac{\partial f^{VMHNC}(\beta,\rho,\eta)}{\partial\eta} = 0 \tag{6}$$

here f^{VMHNC} is free energy which is given by

$$f^{VMHNC}(\beta,\rho,\eta) = f^{MHNC}(\beta,\rho,\eta) - f_{PY}^{MHNC}(\eta) + f_{CS}(\eta) \tag{7}$$

where $f_{PY}^{MHNC}(\eta)$ is the MHNC reduced Helmholtz free energy of the reference hard-sphere fluid within the PY approximation and $f_{CS}(\eta)$ is the empirical HS Carnahan - Starling Helmholtz free energy. In this work the VMHNC theory has been used [10, 17]. Another inversion scheme which is based on the MHNC equation with the revised bridge function, namely, $B_{expt}(r)$ is then given by

$$\beta\phi_{MHNC}(r) = \beta\phi_0(r) + B_{expt}(r). \tag{8}$$

Here $\beta\phi_0(r)$ is the revised effective pair potential extracted from the HNC equation. The revised bridge function $B_i(r)$, as determined replacing subscripts expt by i using the iterative process as follows,

$$\Delta B_{i+1}(r) = [g_{expt}(r) - g_i(r)] - \ln[g_{expt}(r)/g_i(r)] - \Delta c_{i+1}(r) \tag{9}$$

with the following closure relation which has been originally proposed by Poll, Ashcroft and de Witt for One Component Plasma (OCP):

$$g(r) = g_{expt}(r) \qquad r < R_0 \tag{10}$$

$$c(r) = -\beta\phi_0 + A\frac{e^{-\lambda}}{r} \quad r > R_0 \tag{11}$$

The first term in equation (11) is the MSA equation and the second term is the Yukawa correction term which is used to correct any uncertainties in $c(r)$ for $r > R_0$. A and λ are adjustable parameters which are chosen to enforce continuity in $c(r)$ and its first derivative at R_0. PAD ansatz Eq. (11) has been used to extract the revised bridge function in Eq. (8). $B_i(r)$ is determined at every iteration step by substituting the solution of the coupled equation given by Eqs. (3) and (11) into Eq.

(1). The $c_0(r) = c_{HNC}(r)$ is used as initial input for the first run. Iterations are repeated until the difference $|c_{i+1}(r) - c_i(r)| \langle 10^{-5}$ and an accurate estimate for $B_{expt}(r)$ finally can be obtained. This is so-called MHNC+PAD inversion scheme.

3. Results and discussion

3.1. Inversion of experimental structural data

It is emphasised in the literature [18, 25] that the experimental static structure factors of lithium found by different workers show noticeable discrepancies. In order to extract the pair potentials, we shall use a couple of three different sets of experimental values for the static structure factor of liquid lithium reported in Refs. [29, 30]. The thermodynamic states studied in this work specified by the temperatures and different densities are given in Table .

Table 1. The input data for temperatures and densities.

T(K)	470	526	574	595	725
$\rho(\overset{0}{A}^{-3})$	0.0445	0.0441	0.0438	0.0430	0.0420

We can also find another three sets of x-ray and neutron diffraction measurements for $S_{expt}(k)$ at near the melting point about 470K in Ref. [29]. There are some remarkable discrepancies between these measurements of the structure factor at small k values $k < 1A^{-1}$, both the neutron diffraction data of Ruppersberg and co-workers [31] and Waseda's x-ray data [28] shows a linear behaviour, whereas the x-ray data of Olbrich *et al* [33] point to a quadratic behaviour. Fig. 1 shows the discrepancies between different experimental data in the small-k region.We have also included in the same figure, for comparison, the both MD results of S(k) taken from Refs. [18, 25] as $k \to 0$ have been obtained by assuming a quadratic behaviour of S(k) for small k. The both MD results which the NPA potential (MD+NPA)[18] and the potential proposed by Price, Singwi, and Tosi (PST), (MD+PST) [25,34].The experimental value of $S_{expt}(0)$ as calculated 0.027 for liquid lithium at near the melting point [35]. In this study, for all experimental structural data used in our calculations, the range 0 to 0.4 $\overset{o}{(A)}^{-1}$ was covered by extrapolation between $S_{expt}(k)$ as $k \to 0$ and the smallest wavenumber of experimental data to obtain the limit value of $S(0)$. In the same region, the experimental data has been extrapolated smoothly using the sum of differences between the calculated structure factor $S(k)$ and experimental structure factor $S_{expt}(k)$. Those were weighted as follows to obtain a function F which was minimised

$$F = \sum_{i=1}^{N_p} \left| (S(k_i) - S_{expt}(k_i)) \right| \tag{15}$$

here,

$$S(k_i) = S(0) + \exp(\lambda_1 k_i - \lambda_2)\sqrt{k_i} + \lambda_3 k_i^2 \tag{16}$$

where λ_1, λ_2 and λ_3 are constants. N_p is the number of data points in small-k region of $S_{expt}(k)$ which depends on the experimental structure data of liquid lithium used. The values of $S(0)$ deduced in this way are found to be a good agreement with those calculated from the experimental isothermal compressibility data $S_{expt}(0)$ of Ref. [35]. For the large-k region, $S_{expt}(k)$ has been extrapolated to 80 (Å)$^{-1}$ using cubic spline functions to obtain $g(r)$ accurately in the small-r region.

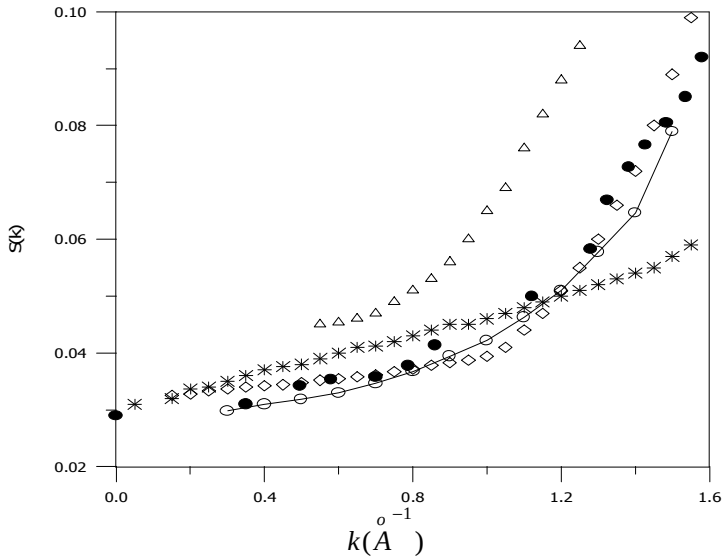

Fig. 1. The small k behaviour of S(k) for liquid lithium at near its melting. The open circles with solid line and solid circles denote the MD+NPA and MD+PST results taken from Refs. [18,25], respectively. The asterisks show Ruppersberg *et al*. data [31], open lozenges, Waseda data [32], open triangles, Olbrich *et al.* [33].

The iterative transform has continued until the direct transform of the $S(k)$ leads to a $g(r)$ that is very flat below r_0, determined by the closest approach of two atoms. In our calculations, we have used the fast Fourier transform routine. The number of grid points are 4096 and step size $\delta r = 0.072\, a_0$ used in numerical integration. It should be noted that the values of modified S(k) are the same as the original experimental data $S_{expt}(k)$ in the small-k region. Concerning the modified structure factors S(k), the main peak of the extracted $S(k)$ becomes lower and broader with decreasing density. As for the pair distribution $g(r)$ with decreasing density, the main peak height becomes lower, while its position remains almost unchanged. We find overall good agreement between the calculated and deduced g(r)'s. We note , however, that the height of the main peak in the calculated VMHNC g(r)'s using the NPA potential are systematically higher than those deduced from experimental data, as pointed out by Gonzalez *et al.* [24] for liquid lithium at near the melting point. But Canales *et al.* has been noted that the MD results of S(k) using the NPA potential at the same thermodynamic state were in good agreement with the experimental data and only small discrepancies observed around the second S(k) maximum. Further, in the long wave limit scaled values of $S^*(0) = 24(2)^{1/2}\int (g(r^*)-1)r^{*2}\,dr^*$ where $r^* = r/r_m$, r_m refers to the position of the first $g(r)$ peak. Due to the good scaling behaviour of $g(r)$, we expect that $S^*(0)$ is constant for liquid Li near melting. The calculated $S^*(0)$ values are in good agreement with others [36]. The average value of $S^*(0)$ from proposed the VMHNC based inversion procedure is 0.45 that is higher than the value of 0.443 from [36] and the calculated value of 0.431 from NPA+VMHNC which means that pair structures were

calculated from the VMHNC, using the pair interaction derived from the NPA. It is expected that the effective pair potentials of lithium should also scale reasonably.

3.2. Effective pair potentials

In this section, we show the revised effective pair potentials for liquid lithium at the thermodynamic states considered in Table. The scaled revised pair potentials $\beta\phi(r)$ for liquid lithium at T=470K, obtained by the VMHNC and MHNC based inversions from the data of Ruppersberg *et al*. [31] are shown in Fig. 2, along with the corresponding pair distribution function obtained by the FT of the extrapolated experimental structure data, scales when they are plotted against r^*.

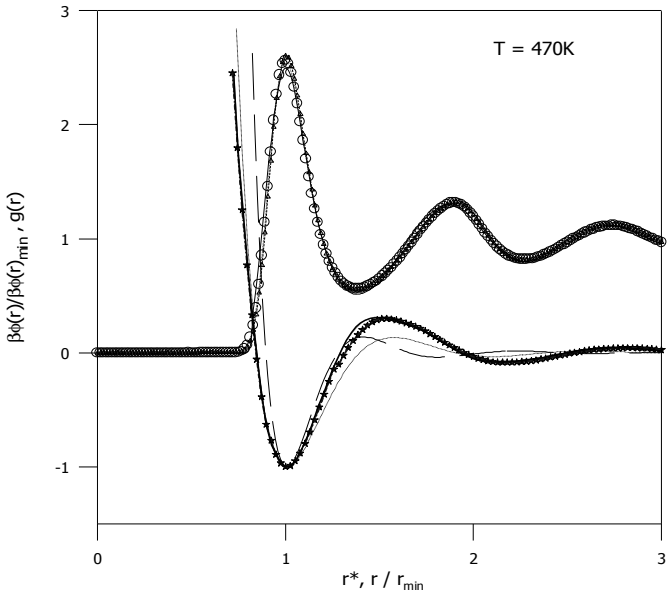

Fig. 2. The scaled pair potentials for liquid lithium at 470K along with the corresponding pair distribution function g(r) vs. *r** Solid lines show VMHNC based revised potentials from the data of Ruppersberg *et al.* [31] and corresponding g(r)'s, stars denote MHNC+PAD revised potentials obtained from the same experimental data. The long-dashed line shows Fiolhais *et al.* Pseudopotential. The dashed line and open circles de note NPA potentials and NPA+VMHNC g(r)'s, respectively.

We also compare these potentials with those obtained from the NPA theory by Gonzalez *et al.* [24] and the second order perturbation theory using a new local pseudopotential proposed by Fiolhais and co-workers [26], along with the corresponding pair distribution function g(r) calculated from VMHNC.

Although we have not included the other revised potentials extracted from the other experimental data to avoid the figures becoming cramped, the comments below take these potentials into account. The presented pseudopotential is the individual choice of Fiolhais and co-workers potential which has been computed using the local density approximation (LDA) version of the local-field factor with the correlation energy of Vosko, Wilk, and Nussair [37]. It may be observed in Fig. 2 that our MHNC based revised potential with revised bridge function is in good agreement with the NPA potential than VMHNC based one. This discrepancy is interpreted as the difference between the parameterized bridge function and the extracted bridge function in the intermediate range distances. Note that, the intermediate-range part of the bridge function depends on the details of the pair potential used in the inversion, resulting in a discrepancy in the intermediate-range part of the g(r)'s obtained by the integral equation and Fourier transformed of the experimental S(k) data. In the presented MHNC+PAD inverse calculations the extracted bridge function is found to be sensitive to the

distance R_0 in Eq. (11). We have taken R_0 = 4.01 Å, A and λ parameters are calculated from the equality of two Eqs. (1) and (8) when B(r)=0. $g_{expt}(r)$ data is discarded outside the distance R = 9.74 Å in the iterative calculations. Concerning the Fiolhais potential, displayed in Fig. 2, agrees quite well with the experimental g(r) deduced from Waseda's data, especially for the position and the height of the peak, except giving the long wavelength limit of the static structure factor of 0.018 compare to the experimental one of 0.027. It is clear that the height of the main peak of g(r) is unimportant for determining $\beta\phi(r)$.

The extracted pair potentials using VMHNC based inversion at two different thermodynamic states of second data set are shown in Fig. 3. It is surprising that our VMHNC results that from the second data set agree well with the NPA potentials, nothing that there is a large difference between two $\beta\phi(r)$.

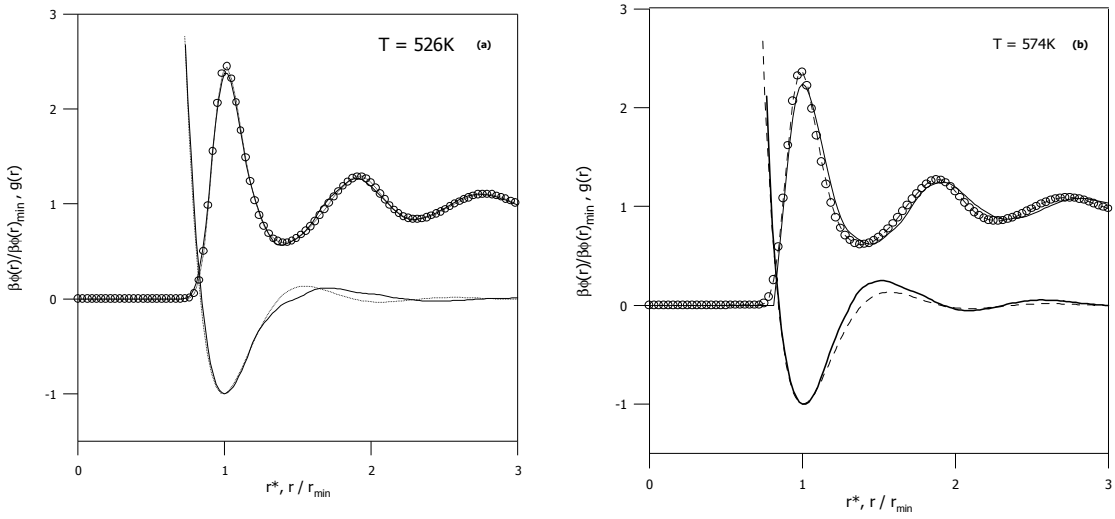

Fig. 3. Comparison of the scaled VMHNC based revised pair potentials for liquid lithium obtained from the experimental data set taken from Ref. [30] at (a) 526 K and (b) 574 K with NPA ones. Same captions as in Fig. 2.

Comparisons of our VMHNC results with the NPA potentials, show that VMHNC inversion scheme gives always shallower potentials at thermodynamic states. It should be noted that VMHNC based potentials show correct trends with decreasing density if the both data sets are taken into account separately.

The scaled revised potentials extracted from the experimental data of the first data set at 725K using the VMHNC inversion are shown in Fig. 4, along with the corresponding g(r) vs. r^* obtained by the FT of the extrapolated experimental structure data. For comparison we have also plotted the scaled potential U(r) of mean force, as $U(r) = k_B T \ln g_{expt}(r)$, and the scaled NPA potential in the same figure. It can be seen that the VMHNC based revised potential agrees quite well with the NPA potential at the long range distances when $\beta U(r)$ and $\beta\phi(r)$ based on VMHNC inversion are excellent agreement at small r. This difference between $\beta U(r)$ and $\beta\phi(r)$ does reflect the direct correlation function c(r), which is related to asymptotic behaviour of $\beta\phi(r)$ at large r. It is clear that the VMHNC inversion scheme corrects these uncertainties in $c(r)$ at long range distances. Since the contribution from the bridge function B(r) is small at low densities, $\beta\phi(r)$ does not depend so much on the approximation for the bridge function in this range.

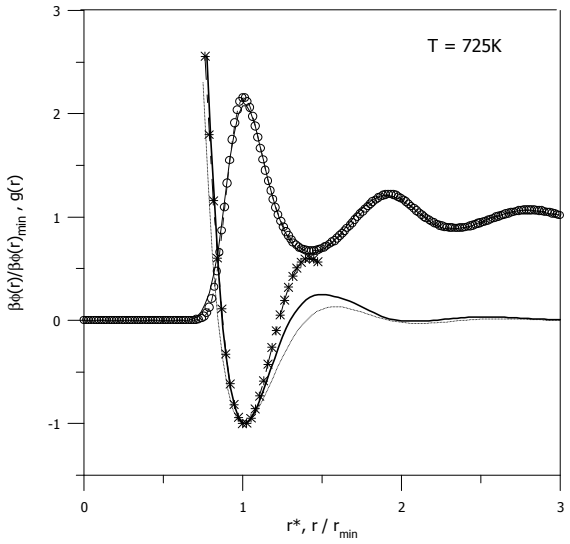

Fig. 4. The scaled revised pair potentials for liquid Li at 725K along with the corresponding $g(r)$ vs. r^*. Same caption as in Fig. 2 for VMHNC based inversions and NPA. Asterisks show the scaled potential U(r) of mean force.

3.3. Thermodynamic properties

We have checked some thermodynamic properties of liquid lithium at the thermodynamic states given in Table. The structural contribution to the internal energy of the metal can be written as

$$\frac{U_{str}}{N} = 2\pi\rho\int_0^\infty r^2\phi(r)g(r)dr\,. \tag{17}$$

The structural part of energy per particle in units of kT($U_{str/NkT}$) is denoted by u_{str}. A similar contribution can be performed for the free energy f, say, f_{nl} is such that $f_{nl} = u_{nl}$. f is the Helmholtz free energy per particle in units of kT (F/NkT). The total entropy per particle in units of k (S/Nk) will be given by

$$s = s_{id} + s_{eg} + s_{str} \tag{18}$$

The electron gas entropy s_{eg} is defined as ,

$$s_{eg} = (mkT/\hbar^2)(\pi Z/9\rho^2)^{1/3} \tag{19}$$

where m is the electron mass and $\hbar$ is Planck's constant. The trends of thermodynamic properties of liquid lithium with temperature are shown in Fig. 5. The structural part of internal energy u_{str} (in NkT units) and excess entropy s^e (in Nk units) calculated from the VMHNC inversion scheme at several temperatures are given comparing with those obtained from NPA+VMHNC method. We also give a comparison of the calculated excess entropies with experimental data taken from Ref. [29] in the same figure. We believe that both data set should be compared separately with NPA. It is seen that in Fig. 5, the values of u_{str} for the first data set, namely at 470K, 595K and 725K show the correct trends for the characteristic features of the density dependence of the VMHNC inverted potentials. They are good agreement with those obtained from NPA+VMHNC . The repulsive part of

$\beta\phi(r)$ becomes softer and the attractive part of the potential becomes weaker and longer ranged as density decreases. It can be easily seen the same trends for u_{str} of the second data set. Comparing the excess entropies with NPA ones shows that VMHNC inversion scheme gives more accurate results. The excess entropy s^e is very important thermodynamic quantity for testing the quality of a given inter atomic interaction.

Finally, it is safe to say that the single-step VMHNC inversion method performs well for liquid Li at presented thermodynamic states, except near its melting. We suggest the MHNC+PAD inversion scheme for liquid metals at their melting points. However the difference between the parameterised bridge function and revised bridge function at short distances might be a cause of concern for other liquid metals near their melting points. The aim of this paper is not to provide a deeper insight on the behaviour of the bridge function in liquid metals at their melting. Calculations by the presented MHNC+PAD procedure are now undertaken for testing the applicability of the inversion scheme for different liquid metals.

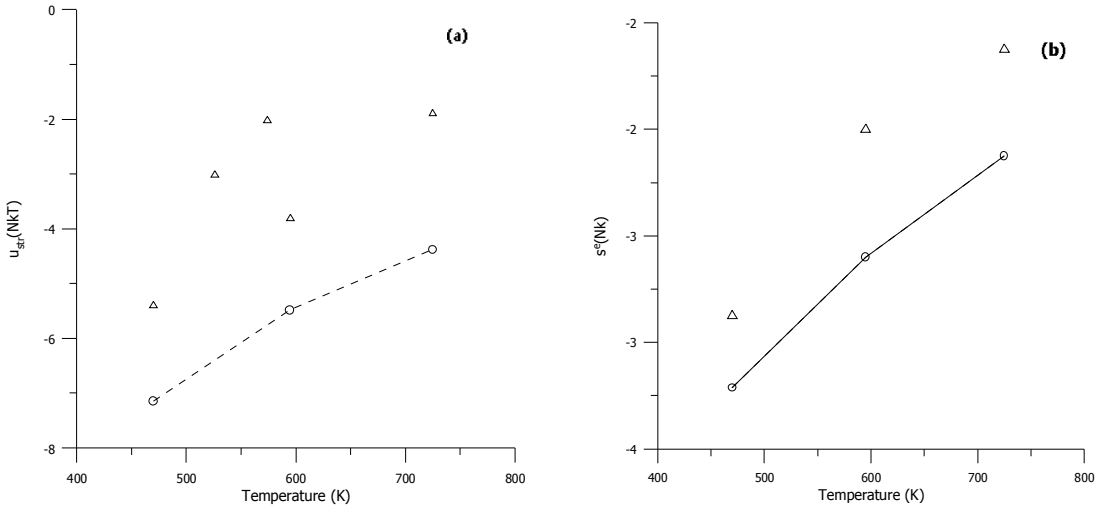

Fig. 5. Variation of the structure part of internal energy u_{str} (in NkT units) (a) and excess entropy s^e (in Nk units) (b) of liquid lithium. Open triangles denote u_{str} and s^e results from present work., open circles with dashed line show NPA+VMHNC results for u_{str} and s^e, solid line, experimental data for excess entropy taken from Ref.[29].

Acknowledgements

We thank L.E. Gonzalez and D. J. Gonzalez for providing us with data prior to publication and discussion on all aspects of this work.

References

[1] M. D. Johnson, N. H. March, Phys. Lett. **3,** 313 (1963).
[2] M. D. Johnson, P. Hutchinson, N. H. March, Proc. R. Soc. London **A282,** 283 (1964).
[3] U. de Angelis, N. March, Phys. Lett. **A56** (1976) 287; Phys. Chem. Liquids **6**, 225 (1977) N. H. March, Can. J. Phys **65,** 219 (1987).
[4] U. Dahlborg, M. Davidovic, Phys. Chem. Liq **15,** 243 (1986); N. H. March, Physics of Simple Liquids, Chap. 15, (North-Holland, Amsterdam, p 645 (1968); D. I. Page, U. de Angelis, N. March, Phys. Chem. Liq. **12,** 53 (1982).
[5] K. Percus, G. L. Yevick, Phys. Rev. **B110,** 1 (1958).
[6] Y. Rosenfeld, N. W. Ashcroft, Phys. Rev. **A20,** 1208 (1979).

[7] L. Reatto, D. Levesque, J. J. Weis, Phys. Rev. **A33,** 3451 (1986).
[8] G. C. Aers, M. W. C. Dharma-wardana, Phys. Rev. **B29,** 2734 (1984).
[9] F. Lado, Phys. Lett. **A89,** 196 (1982), F. Lado, S. M. Foilesand, N. W. Ashcroft, Phys. Rev. **A28,** 237 (1983).
[10] Y. Rosenfeld, J. Stat. Phys **42,** 437 (1986).
[11] M. C. Bellisent-Funel, P. Chieux, D. Levesque, J. J. Weis, Phys. Rev **A39,** 6310. (1989).
[12] S. Munejiri, F. Shimojo, K. Hoshino, M. Watabe, J. Phys. Soc. Japan **64,** 344 (1995).
[13] G. Kahl, M. Kristufek, Phys. Rev. **E49,** 3568 (1994); G. Kahl, B. Bildstein, Y. Rosenfeld, Phys. Rev. **E54,** 5391 (1996).
[14] L. Reatto, M. Tau, J. Chem. Phys. **86,** 6474 (1987).
[15] Y. Rosenfeld, G. Kahl, J. Phys.: Condens.Matter, L89 (1997).
[16] S. Munejiri, F. Shimojo, K. Hoshino, M. Watabe, J. Phys. Condens. Matter. **9,** 3303 (1997); J. Non-Cryst. Solids **207,** 278 (1996).
[17] L. E. Gonzalez, D. J. Gonzalez, M. Silbert, Physica B **168,** 39 (1991); L. E. Gonzalez, D. J. Gonzalez, M. Silbert, Phys. Rev. **A45,** 3803 (1992); L. E. Gonzalez, A. Meyer, M. P. Iniquez, D. J. Gonzalez, M. Silbert, Phys. Rev. **E47,** 4520 (1993); L. E. Gonzalez, S. Dalgic, D. J. Gonzalez, M. Silbert, J. Non-Cryst. Solids. **205 – 207,** 906 (1996); L. E. Gonzalez, M. Silbert, D. J. Gonzalez, S. Dalgıç, Z. Phys. **B,** 13 (1997).
[18] M. Canales, J. A. Padro, L. E. Gonzalez, A. Giro, J. Phys. Condens. Matter **5** 3095 (1993); M. Canales, L. E. Gonzalez, J. A. Padro, Phys. Rev. **E50,** 3656 (1994); M. Canales, J. A. Padro, J. Phys. Condens. Matter **9,** 11009 (1997).
[19] S. S. Dalgic, S. Dalgic, S. Sengul, M. Celtek, G. Tezgor, J. Optoelectron. Adv. Mater. **3**(4), 831 (2001).
[20] S. S. Dalgic, S. Dalgic, U. Domekeli, J. Optoelectron. Adv. Mater. **5**(5), 1263 (2003).
[21] S. S. Dalgic, S. Dalgic, M. Celtek, S. Sengul, J. Optoelectron. Adv. Mater. **5**(5), 1271 (2003).
[22] H. Kes, S. S. Dalgic, S. Dalgic, G.Tezgor, J. Optoelectron. Adv. Mater. **5**(5), 1281 (2003).
[23] L. E. Gonzalez, Ph. D. Dissertation Universidad de Valladolid (1992); L. Dagens, J. Phys. C Solid State Phys. **5,** 2333 (1972); F. Perrot, Phys. Rev. **A42,** 4871 (1990); F. Perrot, N. H. March, Phys. Rev. **A41,** 4521 (1990); F. Perrot, G. Chabrier, Phys. Rev. **A43,** 2879 (1991).
[24] L. E. Gonzalez, D. J. Gonzalez, M. Silbert, J. A. Alonso, J. Phys. Condens. Matter. **5,** 4283 (1993).
[25] A. Torcini , U. Balucani, P. H. K. de Jong, P. Verkerk, Phys. Rev. **E51,** 3126 (1995).
[26] C. Fiolhais, J. P. Perdew, S. Q. Armster, J. M. McLaren, M. Brajczewska, Phys. Rev. **B51,** 14001 (1995); Phys. Rev. **B53,** 13193 (1996); El M. Tammar, J. F. Wax, N. Jakse, J. L. Bretonnet, J. Non-Cryst. Solids. **250 – 252,** 24 (1999).
[27] P. D. Poll, N. W. Ashcroft, H. E. de Witt, Phys. Rev. **A37,** 1672 (1988).
[28] E. Lomba, M. Alvarez, G. Stell, J. A. Anta, J. Chem. Phys. **97,** 4349 (1992); S.Kambiyashi, J. Chihara, Phys. Rev. E, **50**, 1317 (1994).
[29] W. van der Lugt, B. P. Albas, Handbook of Thermodynamic and Transport Properties of Alkali Metals (Blackwell Scientific, Oxford, 1985), Chap. 5.1., edited Ohse, R. W.
[30] A. Sjolander, Amorphous and Liquid Materials, E.Luscher, G. Fritsch, G. Jacucci (eds.). Dordrecht: Martinus Nijhoff (1987).
[31] H. Reither, H. Ruppersberg, W.Speicher Inst. Phys. Conf. Ser., vol **30**, ed R. Evans, D. A. Greenwood (Institute of Physics, Bristol, 1977) p 133.; H. Ruppersberg, and R. Reiter, J. Phys. F: **12,** 1311 (1982).
[32] Y. Waseda, The Structure of Non-Crystalline Materials (McGraw-Hill, New York, 1980)
[33] H. Olbrich, H. Ruppersberg, S. Steeb, Z. Naturf. A, **38,** 1328 (1983).
[34] D. L. Price, S. Singwi, M. P. Tosi, Phys. Rev. B **2**, 2983 (1970).
[35] K. Hornung, in Handbook of Thermodynamic and Transport Properties of Alkali Metals (Ref. 29)
[36] H. S. Kang, Phys. Rev. B, **60**, 6362 (1999).
[37] S. H. Vosko, L. Wilk, M. Nussair, Can. J. Phys. **58**, 1200 (1980).